Nucleic Acids Research, 2025, **53**, gkaf082
https://doi.org/10.1093/nar/gkaf082
Advance access publication date: 18 February 2025
Chemical Biology and Nucleic Acid Chemistry

Strategic base modifications refine RNA function and reduce CRISPR–Cas9 off-targets

Kaisong Zhang†, Wei Shen†, Yunting Zhao†, Xinyan Xu†, Xingyu Liu, Qianqian Qi, Siqi Huang, Tian Tian *, Xiang Zhou

Key Laboratory of Biomedical Polymers of Ministry of Education, College of Chemistry and Molecular Sciences, Hubei Province Key Laboratory of Allergy and Immunology, Wuhan University, Wuhan 430072, Hubei, China

*To whom correspondence should be addressed. Email: ttian@whu.edu.cn
†The first four authors should be regarded as Joint First Authors.

Abstract

In contrast to traditional RNA regulatory approaches that modify the 2′-OH group, this study explores strategic base modifications using 5-carboxylcytosine (ca5C). We developed a technique where ca5C is transformed into dihydrouracil via treatment with borane-pyridine complex or 2-picoline borane complex, leading to base mutations that directly impact RNA functionality. This innovative strategy effectively manages CRISPR–Cas9 system activities, significantly minimizing off-target effects. Our approach not only demonstrates a significant advancement in RNA manipulation but also offers a new method for the precise control of gene editing technologies, showcasing its potential for broad application in chemical biology.

Graphical abstract

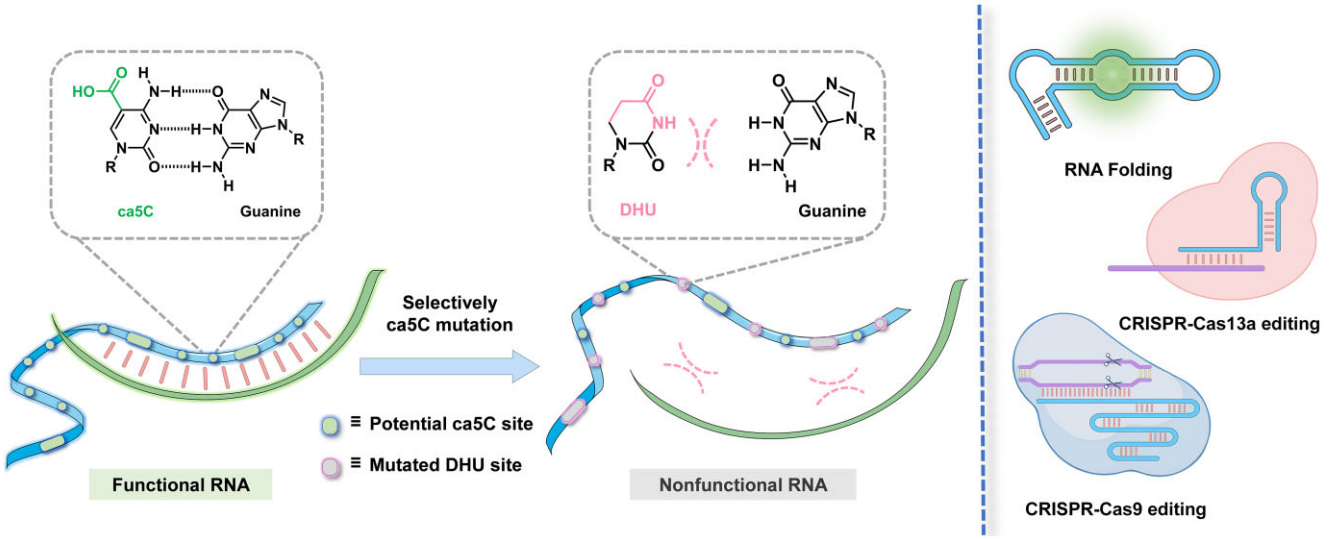

Introduction

RNA is a crucial biomolecule in organisms, playing a vital role in numerous biological functions and regulating physiological processes through its modulation [1, 2]. Developing strategies to control RNA function begins with an understanding of its basic structure [3]. RNA consists of a single nucleoside, which includes ribose and a nitrogenous base [4]. The 2′-OH group on the ribose has been identified as a favorable site for chemical modification, serving as a gateway for introducing various functional groups to RNA [5]. Notable efforts, such as the work on RNA 2′-OH acylation reported by Kool and coworkers, highlight the potential of this approach [3]. Our research has contributed to developing strategies that utilize 2′-OH acylation to modulate RNA function [6–8]. However, we recognize the need for diverse, orthogonal regulatory strategies that can simultaneously regulate different RNA molecules within the same cellular environment to affect various physiological processes. This study focuses

Received: October 13, 2024. **Revised:** January 27, 2025. **Editorial Decision:** January 28, 2025. **Accepted:** January 30, 2025

on the bases of RNA, which are critical for functions such as stem–loop structure formation [9] and molecular hybridization [10]. The challenge lies in innovating ways to endow RNA bases with new functionalities without compromising their original roles, which is the cornerstone of our strategy development.

Our research is particularly focused on epigenetic modifications that preserve the sequence information while enabling new chemical reactions at the base level [11–14]. Various bases undergoing epigenetic modification have been extensively documented [15]. Among these, the TET-assisted pyridine-borane sequencing (TAPS) technology has proven especially intriguing [16]. This technique involves initially oxidizing the methylated cytosine, 5-methylcytosine, to 5-carboxylcytosine (ca5C), which is then converted into dihydrouracil (DHU) using either a borane-pyridine complex (BPC) or 2-picoline borane complex (2-PBC). In sequencing applications, ca5C is read as cytosine (C) and pairs normally with guanine (G). However, DHU pairs with adenine (A) and is read as thymine (T). This peculiar transformation sparked our interest. By introducing ca5C into RNA, it pairs as usual with G, leaving the RNA structure and function unchanged. Subsequent processing with BPC or 2-PBC alters ca5C to DHU, disrupting its usual pairing and hence affecting RNA's original structure and function. This modification strategy offers a promising route to regulate RNA function and activity effectively.

While our previous work demonstrated the impact of f5C on the CRISPR–Cas9 system, it primarily focused on RNA functional modulation and CRISPR gene regulation strategies based on f5C [17]. This study, however, introduces a novel approach using ca5C-based modifications to reduce CRISPR/Cas9 off-target effects, a key difference from our earlier work. Specifically, we show that ca5C modification significantly reduces off-target effects by altering RNA structure, enhancing the precision of gene editing.

In this study, we implemented strategic base modifications to manipulate RNA functionality by incorporating the chemically modified base ca5C into target RNA via *in vitro* transcription. This method specifically replaces select cytosine bases with ca5C, maintaining the rest of the RNA sequence intact. The introduced ca5C is subsequently transformed into DHU through reactions with BPC or 2-PBC, disrupting standard molecular interactions such as hybridization, folding, and enzyme recognition. This alteration was applied to the guide RNA (gRNA) of the CRISPR–Cas9 system, where we demonstrated that the appropriate incorporation of ca5C did not impede the normal CRISPR mechanism. Importantly, this modification provided precise control over the CRISPR–Cas9 editing activity, significantly reducing off-target effects both *in vitro* and in living cells. Our approach, centered on ca5C-directed RNA mutation, offers a versatile tool for refining RNA function across various RNA-dependent systems, enhancing both the accuracy and safety of gene editing applications.

Materials and methods

In vitro transcription and purification of ca5C-containing sgRNAs

Linear DNA templates that contain a T7 promoter sequence upstream of the desired 20–21-bp single guide RNA (sgRNA) protospacer and the sgRNA backbone were obtained by overlap polymerase chain reaction (PCR) (PrimeSTAR HS DNA Polymerase, Takara, #R010A) using the appropriate forward and reverse primers (Supplementary Table S1) and were purified by DNA Clean & Concentrator Kit-5 (Zymo Research, #D4014). The ca5C-containing sgRNA was transcribed with the TranscriptAid T7 High Yield Transcription Kit (Thermo Fisher Scientific, #K0441) at 37°C for 12 h with 75 ng of linear template per 10 μl reaction. 5-Carboxy-CTP (10 mM, TriLink Biotechnologies, #N-1084-5) was mixed with CTP (10 mM) in indicated ratio instead of pure CTP. The RNA products were purified by phenol/chloroform extraction and ethanol precipitation, resuspended in RNase-free H_2O, and stored at −20°C. All RNA sequences are listed in Supplementary Table S2.

Sanger sequencing of the labeled RNA

A consecutive process was conducted to generate complementary DNAs (cDNAs) from ca5C-containing RNAs that were treated with/without borane pyridine, followed by reverse transcription using RevertAid Reverse Transcriptase (Thermo Fisher Scientific, #EP0442) and PCR amplification using PrimeSTAR HS DNA Polymerase. Generated cDNAs were cloned into plasmid vectors using pClone007 Versatile Simple Vector Kit (Tsingke Biotechnology Co., Ltd, 007VS) according to the manufacturer's instructions. Competent DH5α bacteria were transformed with 5 μl ligation mixture and spread onto Luria–Bertani agar plates containing 150 μg/ml ampicillin. Monoclones were picked for Sanger sequencing using an M13F primer (5′-TGTAAAACGACGGCCAGT-3′). C-to-T conversion was analyzed and determined by comparing the peak of C and T by using SnapGene software.

Quantification of ca5C in RNA transcripts

The enzymatic digested products of interested RNA were determined by a two-enzyme cocktail digestion and monitored by high-performance liquid chromatography–mass spectrometry (HPLC–MS). Briefly, 0.4 μg of RNA (with/without borane pyridine treated) transcripts was digested with 100 U S1 Nuclease (Thermo Fisher Scientific, #EN0321) in a 10 μl reaction mixture containing 1× S1 Nuclease buffer (40 mM sodium acetate, 0.3 M NaCl, and 2 mM $ZnSO_4$, pH 4.5, at 25°C). After a 4 h-incubation at 37°C, the mixture was further digested with 0.6 U alkaline phosphatase (Takara, #2660A) in a 50 μl reaction containing 1× AP buffer (50 mM Tris–HCl, 5 mM $MgCl_2$, pH 9.0, at 37°C) to generate each nucleoside. The mononucleosides were separated and detected by using an HPLC–MS (Thermo Scientific Dionex Ultimate 3000 hybrid LTQ Orbitrap Elite Velos Pro) system on a ZORBAX Eclipse XDB-C18 column (2.1 mm × 100 mm, 1.8 μm particle size, 600 bar, Agilent Technologies) in the positive ion multiple reaction monitoring mode. The column temperature was set at 35°C. Formic acid in water (0.1%, solvent A) and formic acid in methanol (0.1%, solvent B) were employed as mobile phase with a flow rate of 0.2 ml/min. A gradient for LC–MS was set as follows: 5% to 80% B over 20 min, 80% B for 7 min, 80% to 5% B over 3 min, and 5% B for 5 min. The contents of the mononucleosides were quantified by comparison with the standard curves that were obtained from nucleoside standards detected at the same time. HPLC–MS (m/z) for ca5C $[M + H]^+$: 272.08 (calculated), 272.08 (found); C $[M + H]^+$: 244.08 (calculated), 244.09 (found); A $[M + H]^+$:

268.10 (calculated), 268.10 (found); G $[M + H]^+$: 284.10 (calculated), 284.10 (found); U $[M + Na]^+$: 267.06 (calculated), 267.06 (found).

GUIDE-seq

For GUIDE-seq study, Cas9-expressing stable cell line HeLa-OC cells, ∼16 h before transfection, were plated on 12-well plates (1.5×10^5 per well) and grown to 70%–80% confluency overnight. Next day, cells were transfected with a total of 120 μl Dulbecco's modified Eagle medium (DMEM) per well: 60 μl DMEM containing 3.5 μl Lipofectamine 3000 (Thermo Fisher Scientific, #L3000015) and 60 μl DMEM containing 1.2 μg sgRNA. Diluted Lipofectamine 3000 and sgRNA were combined and incubated at room temperature for 15 min before slowly adding them to cells. After a 4-h incubation, the medium was changed to complete DMEM and indicated concentrations of BPC were added to the culture media and cells were allowed to incubate for an additional 48 h. Then, cells were washed twice with warm phosphate-buffered saline and genomic DNAs were extracted by FastPure Blood/Cell/Tissue/Bacteria DNA Isolation Kit (Vazyme, #DC112-02) according to the manufacturer's instructions. The diluted genomic DNA products were directly used as a template for PCR amplification of the target region. PrimeSTAR HS DNA Polymerase (Takara, #R010A) was used for amplifying the target site and amplified DNA products were purified using the DNA Clean & Concentrator Kit-5 (Zymo Research, #D4014) according to the manufacturer's instructions. The purified PCR products were digested with 4 U T7 endonuclease I (NEB, #M0302L) in a 10 μl reaction mixture and incubated at 37°C for 60 min. The digested products were separated by a 1.5% agarose gel containing 1.2× Super GelRed (US Everbright Inc., #S2001) for visualization (65 V, 2 h). After quality control analysis, we prepared the genomic DNA from each sample for GUIDE-seq using the protocol reported in the literature [18, 19]. First, genomic DNA was fragmented to ∼300 bp by using Hieff NGS® Fast-Pace DNA Fragmentation Reagent in a one-step process, which was followed by end repair and A-tailing of the fragmented DNA. After that, the processed DNA fragments were ligated to corresponding P5 adapters using T4 DNA ligase. The ligated products underwent two rounds of PCR amplification with Phanta HS Super-Fidelity DNA Polymerase to append P7 adapters with different P7 indexes. The resulting DNA libraries were then sequenced at GENEWIZ, Nanjing. For GUIDE-seq data analysis, we used the open-source guideseq software that is available at https://github.com/aryeelab/guideseq. GRCh37 human genome was used for alignment during the GUIDE-seq analysis procedure (release 44, downloaded from GENCODE, https://www.gencodegenes.org/human/release_44lift37.html), ensuring comprehensive and accurate assessment of the GUIDE-seq results.

On-target ratio was calculated by the following formula:

$$\text{on-target ratio} = \frac{\text{on-target reads}}{\text{on-target reads} + \text{all off-target reads}}.$$

Results and discussion

Designing the ca5C-directed RNA mutation strategy

Our objective is to devise a straightforward and effective method to regulate RNA activity by introducing chemical modifications into RNA bases. These modifications endow RNA with new functionalities without affecting its original functions, enabling it to significantly influence the formation of secondary structures and interactions with other biological macromolecules, such as nucleic acids, proteins, and various small molecules, in response to subsequent stimuli.

Drawing inspiration from TAPS technology [16], our research focuses on manipulating the modified base ca5C, which typically pairs with G and preserves RNA's natural function. However, treatment with BPC and 2-PBC transforms ca5C into DHU. Unlike ca5C, DHU pairs with A and is recognized as T in sequencing. This base mutation disrupts RNA hybridization and secondary structure [1], subsequently altering its physiological activities and functions as illustrated in Scheme 1. We achieved the incorporation of ca5C into RNA by doping ca5C nucleosides during *in vitro* transcription [11, 12], facilitating the production of longer RNA strands with modifications more efficiently than solid-phase synthesis [20].

Regulating long RNA folding through ca5C-directed base mutations

Our initial step was to confirm the feasibility of the ca5C-directed RNA mutation strategy for incorporating ca5C into RNA. We began by verifying the successful incorporation of ca5C into RNA through *in vitro* transcription facilitated by T7 RNA polymerase. Sanger sequencing results indicated that when all CTP in the transcription mixture was replaced with ca5CTP, all cytosine in the RNA, after BPC treatment, had converted from ca5C to DHU as depicted in Fig. 1A and B. Conversely, when only a portion of the CTP was substituted with ca5CTP, some original cytosine residues were retained, as shown in Supplementary Fig. S3. These results confirmed that our RNA mutation strategy was effectively implemented. Additionally, we analyzed the RNA transcription products before and after BPC treatment to assess RNA digestion outcomes and monitored by HPLC–MS. As shown in Fig. 1C and Supplementary Figs S1 and S2, the results demonstrated that ca5CTP was successfully integrated into RNA and subsequently converted to DHU through BPC treatment, validating our approach.

Next, to assess whether the ca5C-directed RNA mutation strategy influences RNA secondary structure formation and consequently alters RNA function, we utilized RNA aptamer experiments. The pepper RNA aptamer, which can form secondary structures, interacts with HBC to elicit fluorescence [21], as shown in Fig. 1D. We produced a series of pepper RNA variants containing ca5CTP by adjusting the ratio of ca5CTP to CTP during *in vitro* transcription, and subsequently treated these with BPC. The impact of the ca5C-directed RNA mutation on RNA activity was evaluated based on the fluorescence intensity upon HBC binding, detailed in Fig. 1E and F. We conducted orthogonal tests to vary ca5CTP incorporation and BPC concentration. The results showed a significant decrease in fluorescence intensity in peppers containing ca5C bases after BPC or 2-PBC treatment compared to the control group, as illustrated in Fig. 1E and F, and Supplementary Figs S4–S6. This decrease indicates that the base mismatches introduced by the ca5C-directed mutation strategy disrupt proper folding of the peppers, thereby inhibiting their native function. The findings from the RNA aptamer experiments demonstrate that the mismatches caused by the ca5C-directed RNA mu-

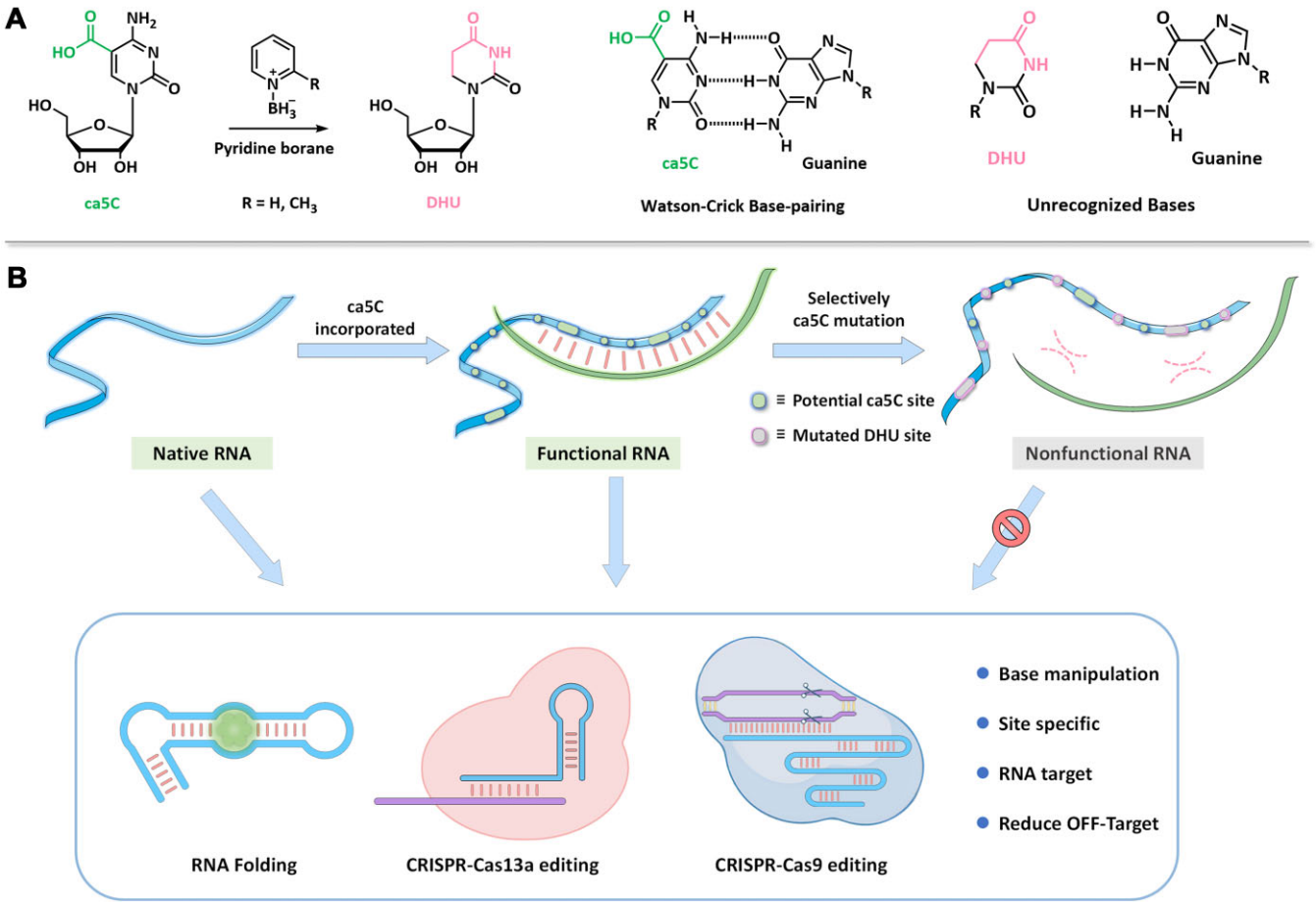

Scheme 1. Design of the ca5C-directed RNA mutation strategy. (**A**) BPC converts ca5C to DHU, inducing base mismatches. (**B**) The ca5C-directed RNA mutation strategy selectively converts ca5C to DHU while preserving cytosine integrity.

tation strategy significantly impact RNA secondary structure formation, which in turn effectively modulates RNA function, particularly in longer RNA sequences.

Regulating CRISPR–Cas9 activity using ca5C-directed RNA mutations

The CRISPR–Cas9 system operates under the guidance of RNA, specifically gRNA, which directs its activity [22]. Overactivity has been a significant challenge in the application of the CRISPR–Cas9 system [23], necessitating effective regulatory strategies. Our ca5C-directed RNA mutation strategy offers a promising method to control the activity of the CRISPR–Cas9 system by modulating RNA function. gRNA exists in two forms: sgRNA and a composite of CRISPR RNA (crRNA) with *trans*-activating crRNA (tracrRNA) [22]. The molecular architecture of the CRISPR–Cas9 system, as reported [24], primarily includes a repeat: anti-repeat duplex and three stem–loop structures that facilitate Cas9 binding (Fig. 2A). We propose that by introducing base mismatches into gRNA, we can disrupt its secondary structure, preventing Cas9 from effectively binding to gRNA. This interference inhibits the overall activity of the CRISPR–Cas9 system, as illustrated in Fig. 2B.

We initially implemented the ca5C-directed RNA mutation strategy in the sgRNA-directed CRISPR–Cas9 system, designing sgRNAs with various sequences to guide cleavage activities for sg-HBEGF [25], sg-HPRT1 [26], and sg-SLX4IP [27]. We discovered that for sg-SLX4IP and sg-HPRT1, activities remained consistent with original sgRNA when ca5CTP occupancy was <60%. However, for sg-HBEGF, activity was unaffected only when ca5CTP occupancy remained below 45% (Supplementary Fig. S7). This indicates that partial replacement of CTP with ca5CTP generally supports CRISPR–Cas9 functionality. Upon establishing that sgRNA containing ca5C could facilitate CRISPR–Cas9 activity, we treated these sgRNAs with BPC and 2-PBC. We observed that BPC and 2-PBC significantly reduced the cleavage activity mediated by ca5C sgRNA, with the inhibitory effect intensifying as the proportion of ca5C in the transcription increased (Fig. 2C and D). The inhibitory impact of BPC and 2-PBC on the CRISPR–Cas9 system also exhibited concentration dependence (Supplementary Figs S9, S11, and S13). Our findings confirm that the ca5C-directed RNA mutation strategy effectively modulates the activity across all three tested sgRNA-mediated CRISPR–Cas9 systems (Fig. 2C and D, and Supplementary Figs S9, S11, and S13), demonstrating its efficacy as a regulatory method for the CRISPR–Cas9 system.

In the sgRNA-mediated CRISPR–Cas9 system, sgRNA is crucial for recognizing target sequences [22]. The presence of potential ca5C-directed sites within sequences that pair with target DNA introduces the risk of sgRNA mispairing with nontarget DNA sequences due to base modifications, potentially leading to novel off-target effects. To circumvent this issue, we explored the crRNA- and tracrRNA-mediated

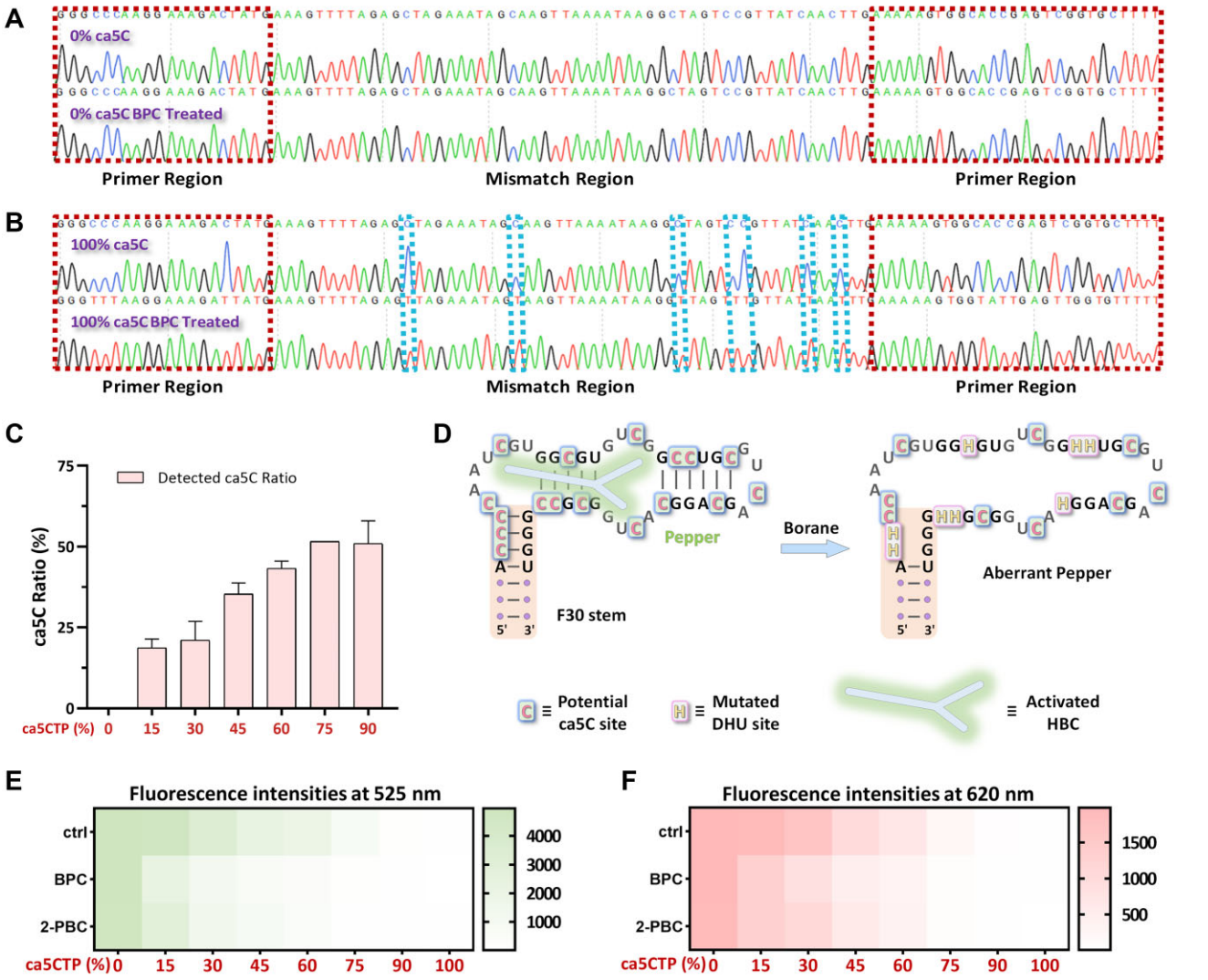

Figure 1. Verification of the ca5C-directed RNA mutation strategy. (**A**) Sanger sequencing results for normal RNA. (**B**) Sanger sequencing results for RNA incorporating ca5C. (**C**) The relative percentage of ca5C incorporation into modified transcripts detected by HPLC–MS. (**D**) Schematic of ca5C-directed base mutation for regulating folding of pepper with (4-((2-hydroxyethyl)(methyl)amino)-benzylidene)-cyanophenylacetonitrile (HBC). (**E**) Heatmap of fluorescence intensities of pepper with different ca5C incorporation ratios with/without BPC (40 mM) or 2-PBC (40 mM) treatment folding with HBC525. (**F**) Folding with HBC620. Color depth within each block represents relative fluorescence intensity.

CRISPR–Cas9 system [22]. In this dual-RNA system, crRNA identifies and pairs with the DNA target site [28], while tracrRNA is essential for forming the ternary complex with crRNA and Cas9 [29, 30]. We thus targeted tracrRNA for the ca5C-directed RNA mutation strategy.

In our studies with the dual-mediated system, we used the same cleavage site as in the sgRNA experiments. We first assessed whether tracrRNA modified with ca5C could function comparably to unmodified tracrRNA. The results indicated high tolerance for ca5C substitution in tracrRNA within the dual system (Supplementary Fig. S8). As anticipated, treatment with BPC and 2-PBC significantly diminished the activity of the CRISPR–Cas9 system mediated by ca5C-tracrRNA and crRNA (Fig. 2E and F). The inhibition by BPC and 2-PBC was concentration-dependent, as demonstrated in Supplementary Figs S10, S12, and S14. Furthermore, the ca5C-directed RNA mutation strategy consistently inhibited the activity of all dual-mediated CRISPR–Cas9 systems we examined (Fig. 2D and F, and Supplementary Figs S10, S12, and S14), mirroring the results observed with sgRNA systems.

After validating that our strategy can be applied to the Cas9 system, we further extended the application of the ca5C mutation strategy to the Cas13a system, an RNA-guided RNA cleavage system, to explore its generalizability. As expected, the ca5C-containing gRNA could efficiently guide Cas13a to cleave the target RNA. However, when treated with BPC/2-PBC to convert it into DHU, Cas13a activity was significantly inhibited, and almost no target RNA was cleaved. Moreover, this inhibition was observed to be concentration-dependent (Supplementary Fig. S22). These results also indicate that the ca5C-directed RNA mutation strategy can be applied to the Cas13a system as well.

ca5C-directed RNA mutations for gene editing regulation

Following the success of the ca5C-directed RNA mutation strategy *in vitro*, we aimed to extend its application to regulate CRISPR–Cas9 activity in living cells. To assess intracellular cleavage efficiency, we employed the T7 endonuclease

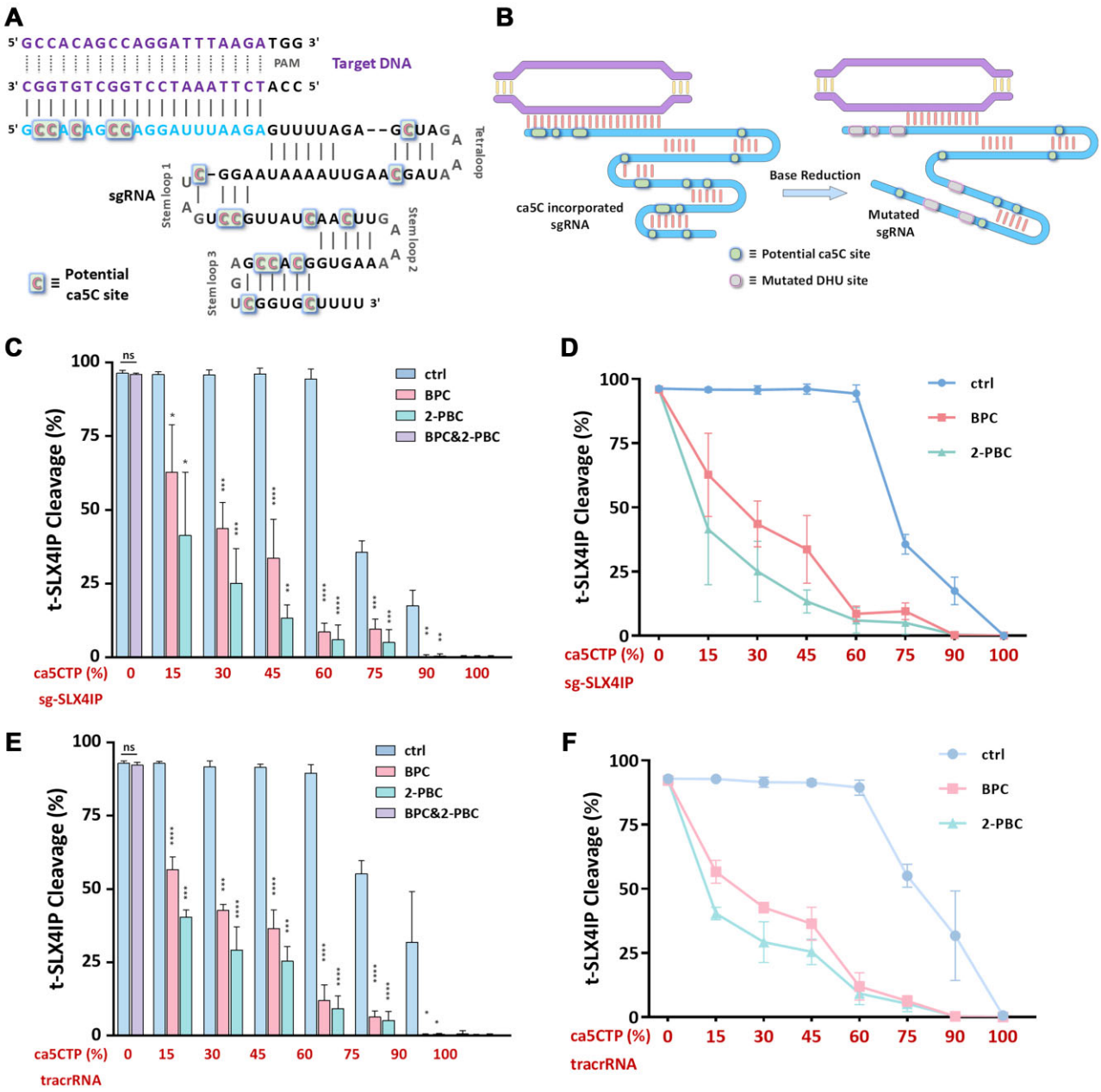

Figure 2. Regulating CRISPR–Cas9 activity using ca5C-directed RNA mutations. (**A**, **B**) Schematic diagrams illustrating the control of the CRISPR–Cas9 system by the ca5C-directed RNA mutation strategy. (**C**) Bar plot showing target cleavage efficiency in the sgRNA-directed CRISPR–Cas9 system under the ca5C-directed RNA mutation strategy. (**D**) Line chart depicting target cleavage efficiency in the sgRNA-directed CRISPR–Cas9 system under the ca5C-directed RNA mutation strategy. (**E**) Bar plot showing target cleavage efficiency in the tracrRNA- and crRNA-directed CRISPR–Cas9 system under the ca5C-directed RNA mutation strategy. (**F**) Line chart depicting target cleavage efficiency in the tracrRNA- and crRNA-directed CRISPR–Cas9 system under the ca5C-directed RNA mutation strategy. The concentrations of BPC and 2-PBC were both 60 mM. Error bars represent average standard error of mean (SEM) from three independent biological replicates. *P*-values are determined by unpaired Student's *t*-test. Source data are provided in a Source Data file. ns (not significant), $P > .05$; $^{*}P < .05$; $^{**}P < .01$; $^{***}P < .001$; and $^{****}P < .0001$.

1 assay [31], which detects mismatched sites in DNA and cleaves them, thereby allowing us to determine the percentage of insertions and deletions (indels) and gauge the editing efficiency of the CRISPR–Cas9 system. Building on our *in vitro* findings, we first conducted a validation experiment in a cell line with stable Cas9 expression [25, 32]. Prior to this, we assessed the cytotoxicity of BPC and 2-PBC to ensure cellular viability (Supplementary Fig. S15) [33, 34].

Next, we investigated the tolerance of ca5C substitution in sgRNA by the CRISPR–Cas9 system in living cells, particularly focusing on the impact of elevated ca5C levels on system efficiency. Our findings revealed that excessive ca5C significantly compromised the performance of the CRISPR–Cas9 system *in vivo*, as shown in Supplementary Figs S16 and S17. Consistent with *in vitro* results, BPC and 2-PBC effectively inhibited ca5C-sgRNA-mediated CRISPR–Cas9 activity, leading to a notable reduction in indels across all experimental groups compared to controls, as illustrated in Supplementary Figs S18 and S21. The inhibitory effects of BPC and 2-PBC were concentration-dependent and effective

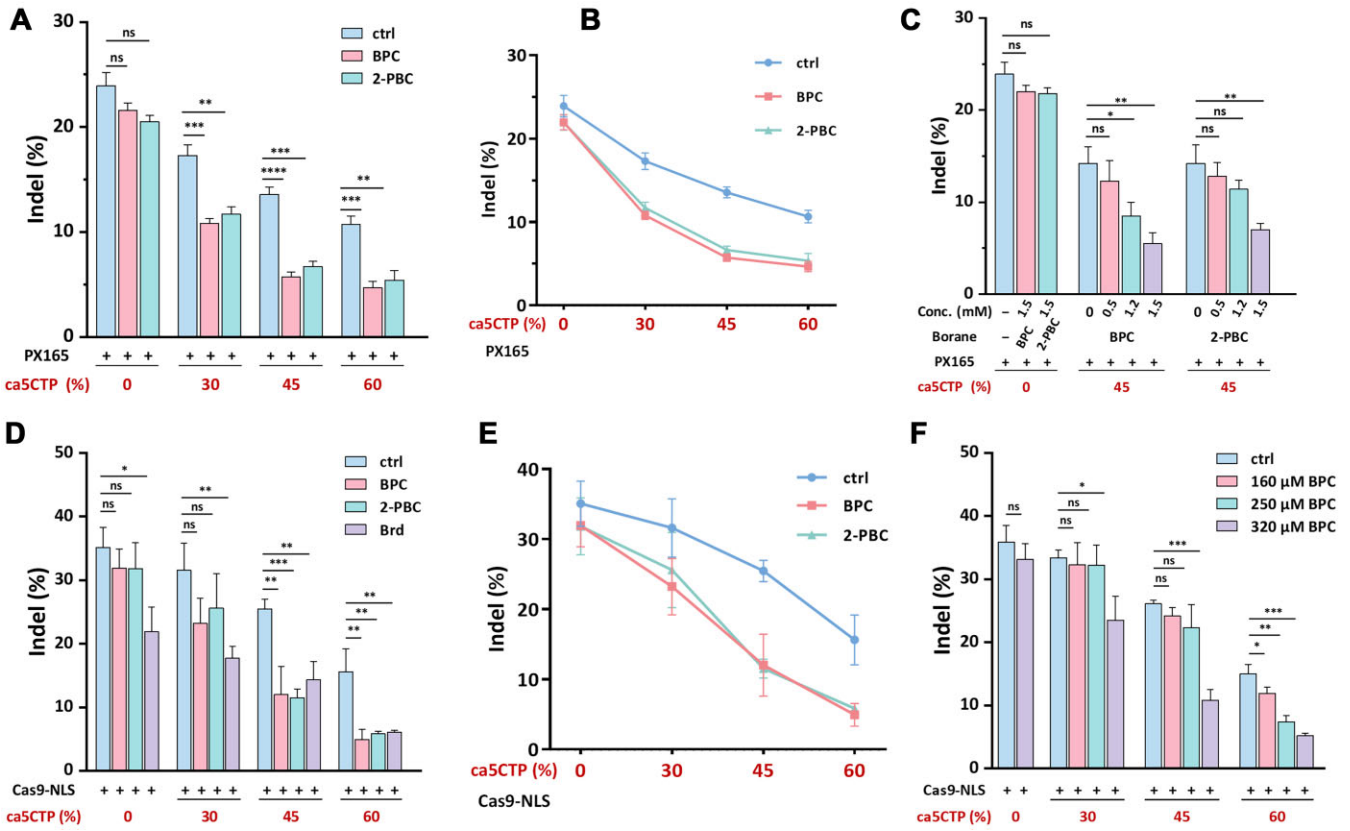

Figure 3. Ca5C-directed RNA mutations for gene editing regulation. (**A**) Bar plot showing editing efficiency of ca5C-incorporated sg-SLX4IP with varying levels of incorporation in PX165 transfected HeLa cells. (**B**) Line chart depicting editing efficiency trends of ca5C-incorporated sg-SLX4IP at increasing incorporation levels in PX165 transfected HeLa cells. The concentrations of BPC and 2-PBC were both 1.5 mM. (**C**) Bar plot of editing efficiency of ca5C-incorporated sg-SLX4IP at 45% ca5CTP in PX165 transfected HeLa cells. (**D**) Bar plot showing editing efficiency of ca5C-incorporated sg-SLX4IP with varying levels of incorporation in RNP transfected HeLa cells. (**E**) Line chart depicting editing efficiency trends of ca5C-incorporated sg-SLX4IP at increasing incorporation levels in RNP transfected HeLa cells. The concentrations of BPC and 2-PBC were both 0.32 mM. (**F**) Bar plot of editing efficiency of ca5C-incorporated sg-SLX4IP in RNP transfected HeLa cells with a gradient of BPC concentrations. Error bars represent average SEM from three independent biological replicates. *P*-values are determined by unpaired Student's *t*-test. Source data are provided in a Source Data file. ns (not significant), $P > .05$; $^{*}P < .05$; $^{**}P < .01$; $^{***}P < .001$; and $^{****}P < .0001$.

at concentrations well below the maximum tolerated by the cells (Supplementary Fig. S15), demonstrating their potential for precise modulation of gene editing processes.

In situations where CRISPR–Cas9 gene editing is required in cell lines that do not stably express Cas9, introducing both Cas9 and sgRNA into cells becomes necessary [35]. Common methods for this include the delivery of Cas9 protein/sgRNA ribonucleoprotein (RNP) complexes [36] and the use of plasmids to express Cas9 (e.g. px165) alongside sgRNA transfection [37], among others [38]. We initially tested plasmid-based delivery methods. As anticipated, sgRNA incorporating ca5C substitutions functioned effectively under this system, albeit with slightly reduced efficiency compared to unmodified sgRNA, as indicated in Supplementary Figs S16 and S17. Our results align with previous findings, demonstrating that the ca5C-directed RNA mutation strategy effectively controls CRISPR–Cas9 editing in living cells using plasmid-based approaches, and the inhibitory effects of BPC and 2-PBC were also concentration-dependent. Notably, both BPC and 2-PBC had only a minor impact on editing efficiency when using conventional sgRNA (Fig. 3A–C and Supplementary Figs S19 and S21). This confirms that alterations in gene editing efficiency are solely attributed to the ca5C-directed RNA mutation strategy. In this particular study, BPC exhibited superior control over gene editing compared to 2-PBC.

The RNP complex strategy offers a more direct approach than plasmid-based methods [38]. Initially, we evaluated whether sgRNA containing ca5C substitutions could function effectively within the RNP framework. Consistent with earlier studies, sgRNA modified with ca5C was operational, albeit slightly less effective than unmodified sgRNA, as evidenced in Supplementary Figs S16 and S17. As anticipated, both BPC and 2-PBC successfully moderated gene editing impacts, markedly reducing editing efficiency (Fig. 3D–F and Supplementary Fig. S20). Additionally, we compared the inhibitory effects of our ca5C-directed RNA mutation strategy with the reported Cas9 inhibitor Brd0539 [39]. While Brd0539 proved more effective with sgRNA containing a low percentage of ca5C, BPC and 2-PBC showed superior inhibition in sgRNA with a high ca5C content (Fig. 3D).

Reducing CRISPR–Cas9 off-target effects in living cells with ca5C-directed RNA mutations

The overactivation of the CRISPR–Cas9 system and the resultant off-target effects present significant challenges for CRISPR–Cas9 gene editing [40, 41]. We have shown that the ca5C-directed strategy can effectively modulate the activity of CRISPR–Cas9. We posit that by mitigating the activity of CRISPR–Cas9, the ca5C-directed RNA mutation strategy

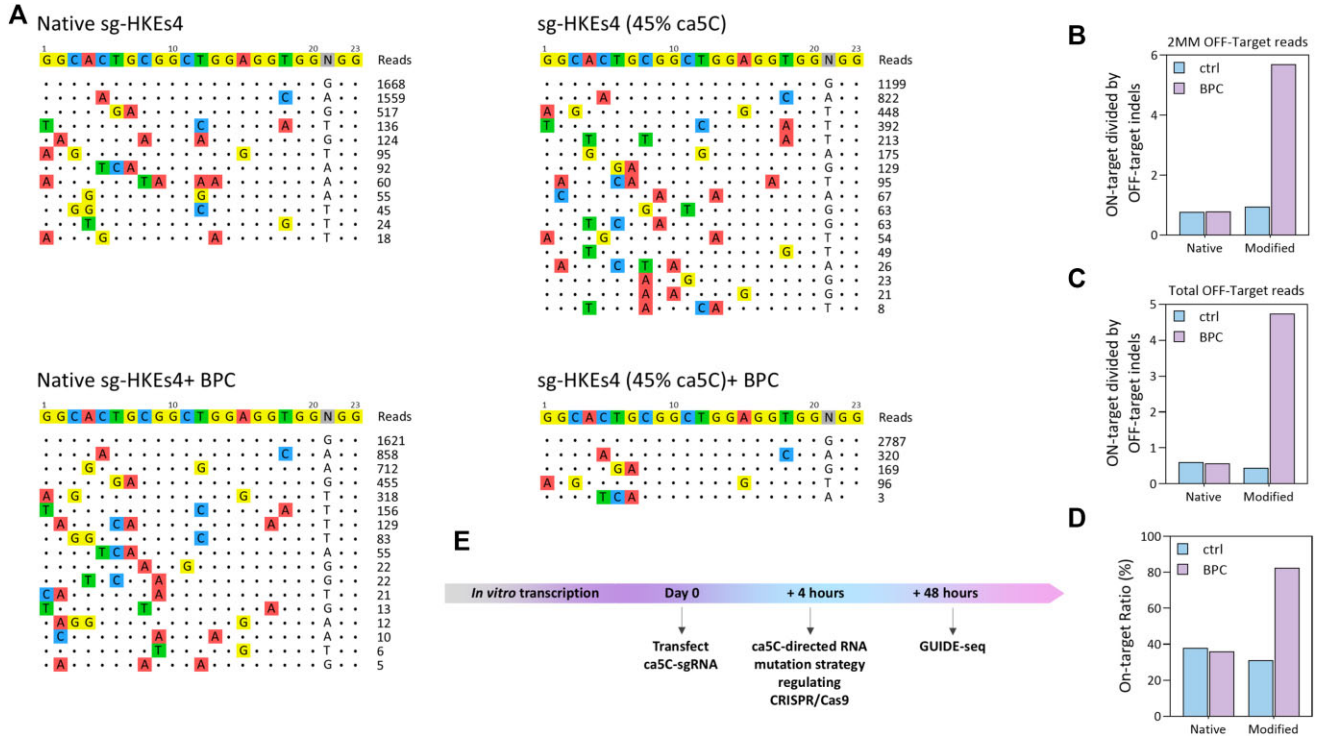

Figure 4. Reducing CRISPR–Cas9 off-target effects in living cells with ca5C-directed RNA mutations. (**A**) GUIDE-seq results comparing native sg-HEKs4 and ca5C-incorporated sg-HEKs4. (**B**) Ratio of on-target indels to 2MM off-target indels. (**C**) Ratio of on-target indels to total off-target indels. (**D**) On-target ratio comparison between native sg-HEKs4 and ca5C-incorporated sg-HEKs4. (**E**) Schematic of the GUIDE-seq process.

can substantially reduce unintended editing outcomes. Currently, the primary techniques for assessing CRISPR–Cas9 off-target effects include GUIDE-seq [18], CIRCLE-seq [42], and CHANGE-seq [43]. Of these, GUIDE-seq is capable of detecting off-target effects in living cells, whereas CIRCLE-seq and CHANGE-seq are limited to *in vitro* assessments.

In this study, we utilized GUIDE-seq to detect the off-target effects of our ca5C-directed strategy. We specifically examined HEK293T site 4 (HEKs4), a location known for its significant off-target issues as identified by Tsai *et al*. in their original report on GUIDE-seq [18]. The ca5C-directed sgRNA-mediated CRISPR–Cas9 gene editing system demonstrated a notable reduction in off-target effects compared to the traditional sgRNA-mediated system (Fig. 4). GUIDE-seq analysis revealed considerable improvements at 2MM (two site mismatch) sites (Fig. 4B), with fewer off-target site types and a reduced percentage of off-target reads observed in the ca5C-directed system. These findings validate our hypothesis that the ca5C-directed RNA mutation strategy effectively minimizes the off-target effects of CRISPR–Cas9 gene editing in living cells.

To further investigate how the ca5C mutation strategy reduces off-target effects, we performed an electrophoretic mobility shift assay (EMSA) experiment to examine the binding of sgRNA to the Cas9 protein. In this experiment, dCas9 was used instead of Cas9. The results demonstrated that the ca5C mutation strategy significantly affected the interaction between sgRNA and the Cas9 protein (Supplementary Fig. S23). We hypothesize that this effect is due to base mismatches caused by ca5C incorporation, which disrupts the proper secondary structure of the sgRNA, thereby impairing Cas9's ability to recognize the sgRNA and ultimately suppressing its activity. When the overall activity of the Cas9 system is suppressed, cleavage of nontarget genes is inhibited, and only those target sequences with minimal mismatches are efficiently cleaved. This mechanism helps to reduce off-target effects. The controlled CRISPR–Cas9 system, guided by this strategy, exhibits substantially fewer off-target effects than the conventional system, addressing a critical challenge within the field. Minimizing these unintended consequences holds profound implications for the clinical application of the CRISPR–Cas9 system.

Discussion

This study demonstrates a novel approach to RNA function modulation using ca5C-based modifications [11, 12], highlighting its profound impact on the sgRNA–Cas9 protein complex integral to the CRISPR–Cas9 system. Effective Cas9 function hinges on precise recognition and binding to specific sgRNA structures [24]. Alterations introduced by ca5C modifications, particularly without BPC or 2-PBC treatment, subtly change sgRNA structure, diminishing its interaction with Cas9 and thereby reducing the overall activity of the CRISPR–Cas9 system. This effect becomes markedly pronounced following treatment with BPC or 2-PBC, which further hampers sgRNA's ability to adopt essential secondary structures. Notably, our study, supported by GUIDE-seq results, suggests that such single-mediator modifications lead to a substantial decrease in off-target effects compared to traditional sgRNA. In addition, our findings from EMSA experiments indicate that the ca5C-induced modifications in sgRNA also significantly impact its binding efficiency with Cas9, which further corroborates our hypothesis that ca5C acts by destabilizing the Cas9–sgRNA complex. We hypothesize that this perturbation reduces cleavage of nontarget genes and enhances speci-

ficity by efficiently cleaving only target sequences with minimal mismatches, thereby reducing off-target effects.

The versatility of the ca5C-directed strategy extends beyond the CRISPR–Cas9 system, indicating its potential applicability to any biological system reliant on the intricate secondary structures of RNA. In this study, we also extended our approach to the Cas13a system, an RNA-guided RNA cleavage system, demonstrating that the ca5C mutation strategy can similarly modulate RNA interactions in this context, further supporting the broad applicability of our method. This method's broad utility is complemented by our development of small-molecule approaches that regulate RNA activity orthogonally to the ca5C strategy. This orthogonality proves invaluable when simultaneous gene editing across multiple targets is required, allowing for targeted regulatory applications specific to each sgRNA. Unlike Cas9 inhibitors, which nonselectively deactivate all CRISPR activities—akin to a master electrical switch—our strategy offers selective control, analogous to individual switches in a parallel circuit, enabling precise manipulations without broad system deactivation.

Moreover, our results suggest that the ca5C-based modifications can be further optimized by combining them with other specificity-enhancing strategies, which could help mitigate the trade-off between overall system activity and target specificity. The balance between these factors is a major challenge in CRISPR technology, and future studies should focus on refining this balance for more efficient gene editing.

While our approach allows for the generation of longer RNA strands more readily than conventional solid-phase synthesis, it lacks the capability to precisely localize modified bases within the RNA sequence. Despite demonstrating the ca5C strategy's effectiveness, we must also consider its interactions with naturally occurring ca5C-modified bases. Although these interactions are infrequent, the broad activity spectrum of BPC and 2-PBC treatments could unintentionally affect normal physiological processes. This highlights the necessity for cautious application and further refinement of our method to minimize unintended disruptions in cellular functions. In this regard, future investigations should focus on developing more targeted approaches to restrict the action of BPC/2-PBC treatments to specific cellular contexts, thereby minimizing the impact on endogenous RNA modifications.

In summary, the combination of ca5C modification and chemical treatment offers an innovative and efficient solution for RNA function modulation and CRISPR system optimization. Future optimization and technological integration will further enhance its potential applications in gene editing and RNA biology research.

Acknowledgements

Author contributions: T.T. and X.Z. conceived the original idea, designed the studies, and led the project. K.Z., W.S., Y.Z., X.X., X.L., Q.Q., and S.H. performed all biological studies. T.T. wrote the manuscript. All the authors provided feedback on the study and on the manuscript. The authors declare no competing financial interests.

Supplementary data

Supplementary data is available at NAR online.

Conflict of interest

None declared.

Funding

This work was supported by the National Natural Science Foundation of China (grants 22177089, 22377094, 22037004, 91853119, 91753201, 22177088, and 22377095) and the Fundamental Research Funds for the Central Universities (grant 2042023kf0204). Funding to pay the Open Access publication charges for this article was provided by National Natural Science Foundation of China (grant 22177089).

Data availability

The data underlying this article are available in the article and in its online supplementary material.

References

1. Armitage BA. Imaging of RNA in live cells. *Curr Opin Chem Biol* 2011;**15**:806–12. https://doi.org/10.1016/j.cbpa.2011.10.006
2. Velema WA, Kietrys AM, Kool ET. RNA control by photoreversible acylation. *J Am Chem Soc* 2018;**140**:3491–5. https://doi.org/10.1021/jacs.7b12408
3. Kadina A, Kietrys AM, Kool ET. RNA cloaking by reversible acylation. *Angew Chem Int Ed* 2018;**57**:3059–63. https://doi.org/10.1002/anie.201708696
4. Voet D, Voet JG. *Biochemistry*. Hoboken, New Jersey, USA: John Wiley & Sons, 2010.
5. Fang LL, Xiao L, Jun YW *et al.* Reversible 2′-OH acylation enhances RNA stability. *Nat Chem* 2023;**15**:1296–305. https://doi.org/10.1038/s41557-023-01246-6
6. Wang SR, Wu LY, Huang HY *et al.* Conditional control of RNA-guided nucleic acid cleavage and gene editing. *Nat Commun* 2020;**11**:91. https://doi.org/10.1038/s41467-019-13765-3
7. Lei HJ, Zeng TY, Ye XF *et al.* Chemical control of CRISPR gene editing via conditional diacylation crosslinking of guide RNAs. *Adv Sci* 2023;**10**:2206433. https://doi.org/10.1002/advs.202206433
8. Qi QQ, Zhang YT, Xiong W *et al.* Norbornene-tetrazine ligation chemistry for controlling RNA-guided CRISPR systems. *Chem Sci* 2022;**13**:12577–87. https://doi.org/10.1039/D2SC02635J
9. Tinoco I, Bustamante C. How RNA folds. *J Mol Biol* 1999;**293**:271–81. https://doi.org/10.1006/jmbi.1999.3001
10. Varshavsky A. Discovering the RNA double helix and hybridization. *Cell* 2006;**127**:1295–7. https://doi.org/10.1016/j.cell.2006.12.008
11. Stengel G, Urban M, Purse BW *et al.* Incorporation of the fluorescent ribonucleotide analogue tCTP by T7 RNA polymerase. *Anal Chem* 2010;**82**:1082–9. https://doi.org/10.1021/ac902456n
12. Steigenberger B, Schiesser S, Hackner B *et al.* Synthesis of 5-hydroxymethyl-, 5-formyl-, and 5-carboxycytidine-triphosphates and their incorporation into oligonucleotides by polymerase chain reaction. *Org Lett* 2013;**15**:366–9. https://doi.org/10.1021/ol3033219
13. Jaenisch R, Bird A. Epigenetic regulation of gene expression: how the genome integrates intrinsic and environmental signals. *Nat Genet* 2003;**33**:245–54. https://doi.org/10.1038/ng1089
14. Mali P, Yang LH, Esvelt KM *et al.* RNA-guided human genome engineering via Cas9. *Science* 2013;**339**:823–6. https://doi.org/10.1126/science.1232033
15. Wang YF, Chen ZG, Zhang X *et al.* Single-base resolution mapping reveals distinct 5-formylcytidine in *Saccharomyces cerevisiae* mRNAs. *ACS Chem Biol* 2022;**17**:77–84. https://doi.org/10.1021/acschembio.1c00633

16. Liu YB, Siejka-Zielinska P, Velikova G *et al.* Bisulfite-free direct detection of 5-methylcytosine and 5-hydroxymethylcytosine at base resolution. *Nat Biotechnol* 2019;**37**:424–9. https://doi.org/10.1038/s41587-019-0041-2
17. Qi Q, Liu X, Fu F *et al.* Utilizing epigenetic modification as a reactive handle to regulate RNA function and CRISPR-based gene regulation. *J Am Chem Soc* 2023;**145**:424–9. https://doi.org/10.1021/jacs.3c01864
18. Tsai SQ, Zheng Z, Nguyen NT *et al.* GUIDE-seq enables genome-wide profiling of off-target cleavage by CRISPR–Cas nucleases. *Nat Biotechnol* 2015;**33**:187–97. https://doi.org/10.1038/nbt.3117
19. Malinin NL, Lee G, Lazzarotto CR *et al.* Defining genome-wide CRISPR–Cas genome-editing nuclease activity with GUIDE-seq. *Nat Protoc* 2021;**16**:5592–615. https://doi.org/10.1038/s41596-021-00626-x
20. Eritja R. Solid-phase synthesis of modified oligonucleotides. *Int J Pept Res Ther* 2007;**13**:53–68. https://doi.org/10.1007/s10989-006-9053-0
21. Chen XJ, Zhang DS, Su N *et al.* Visualizing RNA dynamics in live cells with bright and stable fluorescent RNAs. *Nat Biotechnol* 2019;**37**:1287–93. https://doi.org/10.1038/s41587-019-0249-1
22. Jinek M, Chylinski K, Fonfara I *et al.* A programmable dual-RNA-guided DNA endonuclease in adaptive bacterial immunity. *Science* 2012;**337**:816–21. https://doi.org/10.1126/science.1225829
23. Fu YF, Foden JA, Khayter C *et al.* High-frequency off-target mutagenesis induced by CRISPR–Cas nucleases in human cells. *Nat Biotechnol* 2013;**31**:822–6. https://doi.org/10.1038/nbt.2623
24. Nishimasu H, Ran FA, Hsu PD *et al.* Crystal structure of Cas9 in complex with guide RNA and target DNA. *Cell* 2014;**156**:935–49. https://doi.org/10.1016/j.cell.2014.02.001
25. Zhou YX, Zhu SY, Cai CZ *et al.* High-throughput screening of a CRISPR/Cas9 library for functional genomics in human cells. *Nature* 2014;**509**:487–91. https://doi.org/10.1038/nature13166
26. Ling XY, Chang LY, Chen HQ *et al.* Efficient generation of locus-specific human CAR-T cells with CRISPR/cCas12a. *STAR Protoc* 2022;**3**:101321. https://doi.org/10.1016/j.xpro.2022.101321
27. Panier S, Maric M, Hewitt G *et al.* SLX4IP antagonizes promiscuous BLM activity during ALT maintenance. *Mol Cell* 2019;**76**:27–43. https://doi.org/10.1016/j.molcel.2019.07.010
28. Karvelis T, Gasiunas G, Miksys A *et al.* crRNA and tracrRNA guide Cas9-mediated DNA interference in *Streptococcus thermophilus*. *RNA Biol* 2013;**10**:841–51. https://doi.org/10.4161/rna.24203
29. Chylinski K, Le Rhun A, Charpentier E. The tracrRNA and Cas9 families of type II CRISPR–Cas immunity systems. *RNA Biol* 2013;**10**:726–37. https://doi.org/10.4161/rna.24321
30. Liao CY, Beisel CL. The tracrRNA in CRISPR biology and technologies. *Annu Rev Genet* 2021;**55**:161–81.
31. Sentmanat MF, Peters ST, Florian CP *et al.* A survey of validation strategies for CRISPR–Cas9 editing. *Sci Rep* 2018;**8**:888. https://doi.org/10.1038/s41598-018-19441-8
32. Zhao DX, Badur MG, Luebeck J *et al.* Combinatorial CRISPR–Cas9 metabolic screens reveal critical redox control points dependent on the KEAP1–NRF2 regulatory axis. *Mol Cell* 2018;**69**:699–708. https://doi.org/10.1016/j.molcel.2018.01.017
33. Gavanji S, Bakhtari A, Famurewa AC *et al.* Cytotoxic activity of herbal medicines as assessed *in vitro*: a review. *Chem Biodivers* 2023;**20**:e202201098.
34. Stockert JC, Horobin RW, Colombo LL *et al.* Tetrazolium salts and formazan products in cell biology: viability assessment, fluorescence imaging, and labeling perspectives. *Acta Histochem* 2018;**120**:159–67. https://doi.org/10.1016/j.acthis.2018.02.005
35. Luther DC, Lee YW, Nagaraj H *et al.* Delivery approaches for CRISPR/Cas9 therapeutics *in vivo*: advances and challenges. *Expert Opin Drug Deliv* 2018;**15**:905–13. https://doi.org/10.1080/17425247.2018.1517746
36. Kim S, Kim D, Cho SW *et al.* Highly efficient RNA-guided genome editing in human cells via delivery of purified Cas9 ribonucleoproteins. *Genome Res* 2014;**24**:1012–9. https://doi.org/10.1101/gr.171322.113
37. Ran FA, Hsu PD, Wright J *et al.* Genome engineering using the CRISPR–Cas9 system. *Nat Protoc* 2013;**8**:2281–308. https://doi.org/10.1038/nprot.2013.143
38. Liu C, Zhang L, Liu H *et al.* Delivery strategies of the CRISPR–Cas9 gene-editing system for therapeutic applications. *J Control Release* 2017;**266**:17–26. https://doi.org/10.1016/j.jconrel.2017.09.012
39. Maji B, Gangopadhyay SA, Lee M *et al.* A high-throughput platform to identify small-molecule inhibitors of CRISPR–Cas9. *Cell* 2019;**177**:1067–79. https://doi.org/10.1016/j.cell.2019.04.009
40. Guo CT, Ma XT, Gao F *et al.* Off-target effects in CRISPR/Cas9 gene editing. *Front Bioeng Biotechnol* 2023;**11**:1143157. https://doi.org/10.3389/fbioe.2023.1143157
41. Zhang XH, Tee LY, Wang XG *et al.* Off-target effects in CRISPR/Cas9-mediated genome engineering. *Mol Ther Nucleic Acids* 2015;**4**:e264. https://doi.org/10.1038/mtna.2015.37
42. Tsai SQ, Nguyen NT, Malagon-Lopez J *et al.* CIRCLE-seq: a highly sensitive *in vitro* screen for genome-wide CRISPR–Cas9 nuclease off-targets. *Nat Methods* 2017;**14**:607–14. https://doi.org/10.1038/nmeth.4278
43. Lazzarotto CR, Malinin NL, Li YC *et al.* CHANGE-seq reveals genetic and epigenetic effects on CRISPR–Cas9 genome-wide activity. *Nat Biotechnol* 2020;**38**:1317–27. https://doi.org/10.1038/s41587-020-0555-7

Received: October 13, 2024. **Revised:** January 27, 2025. **Editorial Decision:** January 28, 2025. **Accepted:** January 30, 2025